Circular deformation estimation for a flexible link

J. Vihonen, *Member, IEEE*, P. Mäkinen, J. Mattila, *Member, IEEE*, and A. Visa, *Senior Member, IEEE*

***Abstract*—To address the tip positioning problem among flexible link robotic applications, we propose a new circular beam deformation model that is ideally suited for networked linear accelerometers and rate gyros. Importantly, the tip positioning problem of multiple-flexible-link system is reduced to the tip positioning problem of an individual flexible link subject to the circularly characterized deformation. The validity of the theoretical results is verified by experiments with a highly flexible single-link hydraulic manipulator.**

I. Introduction

Link flexibilities show up inevitably with lightweight or long reach links. For example, this can be seen from the Euler-Bernoulli beam equation: the static deformation of a uniform cantilever beam subject to a force at the free end is proportional to the third power of the beam length [1]. By far, the most successfully designed tip control solutions have been based on either computationally intensive computer vision and/or relatively inaccurate strain gauges, e.g., [2]–[4]. However, low-cost strap-down inertial sensors have been envisioned to offer an attractive alternative to existing sensor solutions, but the majority of this research has focused on stiff structures and rigid body kinematics, see, e.g., [5], [6] and the references therein. A careful literature review reveals that recovering the bending profile by means of inertial sensing of highly flexible structures has not been well developed, apart from few specific cases focused on elasticity at the joints, see [7]–[9].

In this paper, our objective is to estimate the amount of beam bending for advanced motion control schemes using a network of beam-fixed inertial sensors. In Sect. II, we propose a new circular beam deformation model for the fusion of relatively low-resolution linear accelerometers' and rate gyros' readings. By cascading the inertial sensors and describing the bending from one sensor to the other as a circle-shaped closed curve, the model circumvents the drifting issue in the accelerometer reading double integration [10] while keeping assumptions to a minimum. A control implementation with elastic vibration damping capabilities is experimented in Sect. III, where we estimate the local deformations of a 4.5 m flexible link in real time. In this way, we qualify the whole deformation profile of the beam in vertical plane, which is of the most practical interest from the mechanical stress accumulation viewpoint.

II. Deformation characterization

Suppose a beam of length L^0 is actuated by revolute joint in the vertical plane, as illustrated in Fig. 1. The reference frame $\{B_0\}$ is fixed to the ground, and a body frame $\{B_1\}$ is attached to the distal end of the undeformed beam such that its y axis intersects the joint center. To observe any deformation, we have attached sensor frames $\{P_1\}, \ldots, \{P_i\}$ to the beam. The frame $\{P_i\}$ is on the beam tip for ease of illustration.

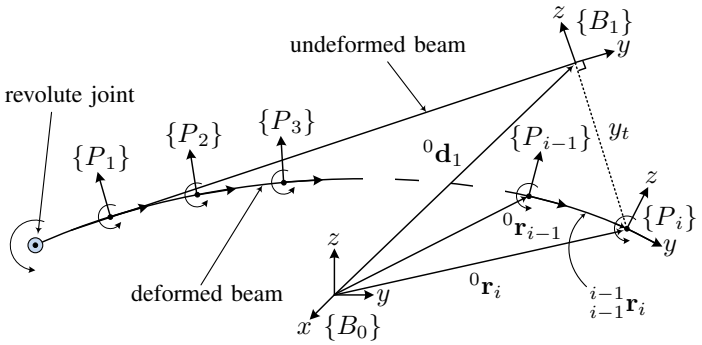

Fig. 1. Sensor frames $\{P_1\}, \ldots, \{P_i\}$ attached to a deformed beam. By associating the sensor frames with accelerometers and rate gyros, we estimate the tip angle and deflection with respect to the undeformed beam tip $\{B_1\}$.

A. New circular beam deformation model

The position vector ${}^0\mathbf{r}_i$ of the frame $\{P_i\}$ can be expressed using a unique rotation and translation:

$$ {}^0\mathbf{r}_i = {}^0\mathbf{r}_{i-1} + {}^0R_{i-1}\, {}^{i-1}_{i-1}\mathbf{r}_i. \tag{1} $$

Here, ${}^0\mathbf{r}_{i-1}$ is the position of frame $\{P_{i-1}\}$ expressed in frame $\{B_0\}$, and ${}^{i-1}_{i-1}\mathbf{r}_i$ denotes the position of frame $\{P_i\}$ with respect to $\{P_{i-1}\}$ expressed in frame $\{P_{i-1}\}$. The orientation of frame $\{P_i\}$, or the tip angle, may be given as

$$ {}^0R_i = {}^0R_{i-1}\, {}^{i-1}R_i, \tag{2} $$

where ${}^{i-1}R_i$ is the orientation of frame $\{P_i\}$ with respect to $\{P_{i-1}\}$. As the beam is rotated by about its longitudinal axis relative to the force of gravity, variation in the amount of beam bending appears, which changes the vector distance ${}^{i-1}_{i-1}\mathbf{r}_i$.

Suppose the original undeformed length between the frames $\{P_i\}$ and $\{P_{i-1}\}$ is denoted by L^0_i, as shown in Fig. 2. The deformed length is denoted by L_i. We model gravity-caused beam deformation shape to be circular:

$$ \theta_i = \begin{cases} -\alpha_i & \text{for } \alpha_i < 0 \\ \alpha_i & \text{otherwise,} \end{cases} \tag{3} $$

where α_i denotes the angle of the arc that can be extracted from the matrix ${}^{i-1}R_i$, i.e., ${}^{i-1}R_i = R(\alpha_i)$. For $\theta_i \neq 0$, the radius of curvature is then

$$ \rho = \frac{L^0_i}{\theta_i} \tag{4} $$

and the law of cosines yields

$$ L_i = \begin{cases} L^0_i & \text{for } \theta_i = 0 \\ \sqrt{2\rho^2 - 2\rho^2\cos(\theta)} & \text{otherwise.} \end{cases} \tag{5} $$

Inserting the above to the Pythagorean theorem

$$ \Delta\rho_i = \rho_i - \sqrt{\rho_i^2 - (0.5L_i)^2} \tag{6} $$

[1]The authors are with Tampere University of Technology, Korkeakoulunkatu 1, FI-33101, Tampere, Finland. E-mail: firstname.surname@tut.fi

gives the displacement in the middle. Moreover, since $\beta_i = 0.5\alpha_i$, we can define

$$ {}^{i-1}_{i-1}\mathbf{r}_i = R(\beta_i)\,[0\ L_i\ 0]^{\mathrm{T}}. \tag{7} $$

Therefore, the vectorized distance ${}^{i-1}_{i-1}\mathbf{r}_i$ may be considered known to a high degree of accuracy, and it follows that

$$ {}^0\mathbf{r}_i = \sum_{j=1}^{i} {}^0R_j\ {}^j_{j-1}\mathbf{r}_j. \tag{8} $$

Hence, the tip deflection with respect to the undeformed beam tip $\{B_1\}$ can be given as

$$ y_t = ||{}^0\mathbf{r}_i - {}^0\mathbf{d}_1||_2, \tag{9} $$

where ${}^0\mathbf{d}_1$ is given by the rigid body kinematics. The frames $\{P_i\}$ and $\{B_1\}$ are coincident in the case of no deformation.

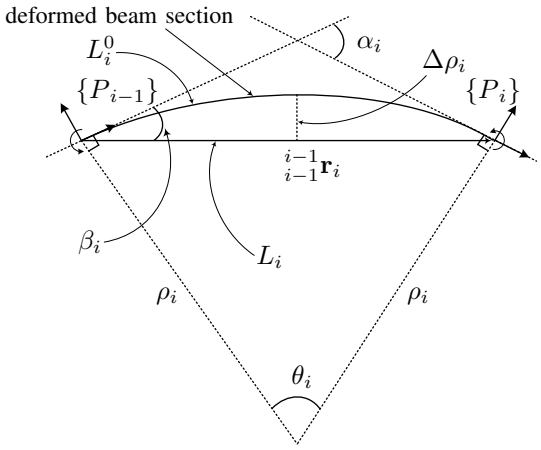

Fig. 2. Circular characterization of gravity-caused beam deformation between sensor frames $\{P_{i-1}\}$ and $\{P_i\}$ assuming constant strain of the beam.

B. Real-time deformation estimation by inertial sensor network

The proposed circular beam deformation model is dependent on the angle of the arc α_i. To estimate it in real-time, suppose a linear 3-axis accelerometer is located at the origin of $\{P_i\}$ to measure accelerations with respect to the inertial frame $\{I\}$.[1] The linear accelerometer output can be expressed by:

$$ {}^i\mathbf{a}_i = {}^i\ddot{\mathbf{r}}_i - {}^i\mathbf{g} + \mathbf{n}_i \in \mathbb{R}^3 \tag{10} $$

where ${}^i\ddot{\mathbf{r}}_i$ denotes the instantaneous accelerations of motion, ${}^i\mathbf{g}$ is the force of gravity acting on the accelerometer, such that $||{}^i\mathbf{g}|| \approx 9.8$ m/s^2, and $\mathbf{n}_i$ is a noise term. Next, by associating a network of accelerometers with frames $\{P_1\}, \ldots, \{P_{i-1}\}$, too, we establish the following relationship

$$ {}^{i-1}\mathbf{a}_{i-1} = {}^{i-1}R_i\Big({}^i\mathbf{a}_i - {}^i_{i-1}\ddot{\mathbf{r}}_i\Big) = {}^{i-1}\mathbf{a}_i \tag{11} $$

where ${}^i_{i-1}\ddot{\mathbf{r}}_i$ denotes the accelerations caused by the displacement of $\{P_{i-1}\}$ and $\{P_i\}$ while in motion. Since ${}^{i-1}R_i = R(\alpha_i)$ now appears in (11), rearranging the terms leads to

$$ \alpha_i^a = \arctan\Big(\frac{{}^{i-1}a_i^y\,{}^{i-1}a_{i-1}^z - {}^{i-1}\,a_i^z\,{}^{i-1}a_{i-1}^y}{{}^{i-1}a_i^y\,{}^{i-1}a_{i-1}^y + {}^{i-1}\,a_i^y\,{}^{i-1}a_{i-1}^z}\Big), \tag{12} $$

[1]For notational convenience, sub- and superscripts "I"are hereafter omitted for quantities referred to the inertial reference frame $\{I\}$.

where the superscripts x, y, and z denote the axial components of (11). However, this estimate is prone to the high accelerometer noise and offsets unless the term ${}^i_{i-1}\ddot{\mathbf{r}}_i$ is reconstructed.

The proposed circular modeling can be utilized for real-time reconstruction of the linear accelerations ${}^i_{i-1}\ddot{\mathbf{r}}_i$ in (12). That is, assuming that the deformation does not effect the total beam length, i.e., $L^0 = \sum_{j=1}^{i} L_j^0$, differentiating (1) twice results in

$$ {}^i_{i-1}\ddot{\mathbf{r}}_i = {}^i\dot{\boldsymbol{\omega}}_i \times {}^i_{i-1}\mathbf{r}_i + {}^i\boldsymbol{\omega}_i \times ({}^i\boldsymbol{\omega}_i \times {}^i_{i-1}\mathbf{r}_i), \tag{13} $$

where ${}^i\boldsymbol{\omega}_i$ denotes the instantaneous angular velocity and ${}^i\dot{\boldsymbol{\omega}}_i$ is the angular acceleration of frame $\{P_i\}$ relative to $\{B_0\}$, respectively. To define the two quantities in practice, suppose the angular velocity of $\{P_i\}$ is sensed by 3-axis rate gyro:

$$ {}^i\boldsymbol{\Omega}_i = {}^i\boldsymbol{\omega}_i + \mathbf{b}_i + \boldsymbol{\mu}_i \in \mathbb{R}^3, \tag{14} $$

where ${}^i\boldsymbol{\omega}_i$ denotes the true angular rate of $\{P_i\}$ with respect to $\{I\}$, a constant or slowly time-varying gyro bias is denoted by $\mathbf{b}_i$, and $\boldsymbol{\mu}_i$ is a noise term. Now, the angular acceleration in (13) can be obtained by the numerical differentiation of (14). Importantly, by differentiating (2) and associating a gyro also with $\{P_{i-1}\}$, we obtain a derivative of the arc angle α_i:

$$ \dot{\alpha}_i^g\,{}^i\hat{k}_{i-1} = {}^i\boldsymbol{\Omega}_i - {}^i\boldsymbol{\Omega}_{i-1} = {}^i_{i-1}\boldsymbol{\omega}_i + \mathbf{b}_i + \boldsymbol{\mu}_i \tag{15} $$

where ${}^i\hat{k}_{i-1}$ is the unit vector of the revolute joint axis. Here, $\mathbf{b}_i$ and $\boldsymbol{\mu}_i$ stand for the coupled biases and noises preventing the open-loop integration of (15), as we shall show.

Because heavy-duty manipulators have almost exclusively 1-DOF joints, we use the following filter to compensate for the high noise in (12) and bias dynamics of (15):

$$ \begin{bmatrix} \hat{\alpha}_i(t) \\ \hat{b}_i(t) \end{bmatrix} = \begin{bmatrix} 1 & T_s \\ 0 & 1 \end{bmatrix} \begin{bmatrix} \hat{\alpha}_i(t-1) \\ \hat{b}_i(t-1) \end{bmatrix} + \begin{bmatrix} T_s & 0.5T_s^2 \\ 0 & T_s \end{bmatrix} \begin{bmatrix} k_1 \\ k_2 \end{bmatrix} \Big(\alpha_i^a - \hat{\alpha}_i(t-1)\Big) + \begin{bmatrix} T_s \\ 0 \end{bmatrix} \dot{\alpha}_i^g, \tag{16} $$

where t denotes time, T_s is the sampling time, and k_1 and k_2 denote the filter's gains. As usual in Kalman filtering, we choose the gains such that $k_1 \gg k_2$ to accommodate the slowly-time varying gyro bias dynamics. We also set the gains close to zero on-line if the beam undergoes high magnitude accelerations ignored by the kinematic model (13), such as shocks.

III. Experimental model validation

To verify the validity of the circular deformation model, experiments were carried out with a hydraulically actuacted 4.5 m long flexible link made of high strength steel and having 60 mm×60 mm×3 mm cross-section in Fig. 3. Equating some three times the mass of the flexible link itself, a load of 70 kg was attached at the tip. A digital encoder of type SICK Stegmann DGS60 was fitted to the rotary joint angle to measure the beam's angle about its axis of rotation. Four inertial units based on ADIS16485 *i*Sensor MEMS module, packing a 3-axis ± 5 g accelerometer and 3-axis ± 450 deg/s gyroscope, were mounted on the link. A PowerPC-based dSpace DS1103 system was used as the real-time control interface to a servo valve, and for sampling of the sensors at 500 Hz rate ($T_s = 0.002$ s).

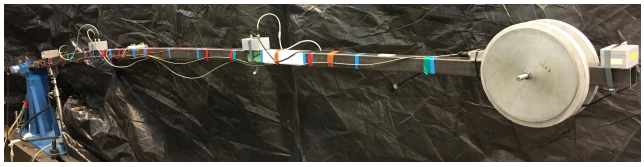

Fig. 3. Hydraulically actuated flexible steel beam with four inertial units. The maximum stress is at the hydraulic cylinder's connection point on left.

Fig. 4 demonstrates our tip angle estimation under free, 1 Hz vibration of the tip. More precisely, three cases are shown: i) the circular deformation model without the real-time acceleration compensation, see (11) and (13), ii) integration of the rate (15) as such, and iii) the full circular deformation model culminating to (16). As can be seen from iii), the proposed estimation remains completely bias free while in fast motion. The result is highlighted by the fact that the link's natural dampening of elastic vibrations is very low, making i) and ii) prone to loss of accuracy and drifting over a considerable period of time.

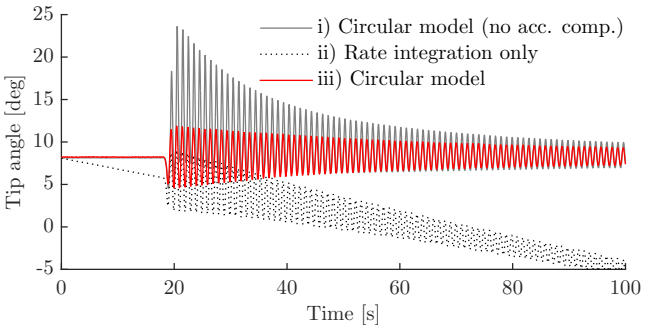

Fig. 4. Gyro bias dynamics and acceleration effects illustrated in tip angle estimation. The circular model remains accurate under free link vibration.

For control purposes, an arc approximation, used for example in [11], was applied as a representation of the tip position:

$$y = L^0\alpha_0 + y_t, \tag{17}$$

where α_0 denotes the rotation angle from the encoder attached to the joint. The use of this approximation is convenient due to the fact that the deflection y_t can be directly obtained from a finite element (FE) model based dynamic observer. The Euler-Bernoulli beam theory (e.g., [1]) was used to derive the dynamic equation of motion. The characteristic elastic modulus and material density values for the steel of the beam were 210 GPa and 7850 kg/m^3, respectively. However, the implementation of FE models into real-time systems is usually not feasible [12], which is why our realization relies on a cantilever beam model comprising only 5 elements. To damp elastic vibrations on the fly, control equations were formulated for the tip angle and tip position (arc length) using the modality presented in [13].

Fig. 5 presents tip deflections with respect to a professional optical tracking system of type OptiTrack:V120 Trio. The link was inclined almost vertically from the horizontal level with the optical tracker tracking its tip. Though some sync errors can be seen, our inertial sensor network provides a bias-free estimate smoothly following the optical reference. However, depending on the inclination, the encoder fixed on the link's rotating axis is constantly off by 15-42 cm, which is reduced to some 6-24 cm by the FE based observer (not shown for clarity). This verifies the validity of the circular beam deformation model.

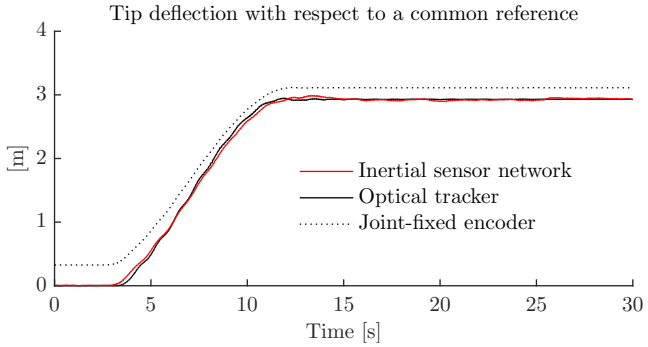

Fig. 5. Tip deflections under elastic vibration damping control. The root mean square error of the circular deformation estimate in respect to the optical reference is only 3.3 cm – a 7-fold improvement over the plain encoder use.

IV. Conclusion

In this paper, the amount of beam bending has been estimated using a new circular deformation model for inertial sensors. Owing to (7), (11), (15) and (16), the model operates on floating base, making it equally applicable to manipulators comprising multiple flexible links in vertical plane. In this way, dynamic modeling efforts often required in the form of rather difficult observer design may be even obviated. This an important milestone to us, to which we do not know a prior reference.

References

[1] W.-H. Zhu, C. Lange, and M. Callot, "Virtual decomposition control of a planar flexible-link robot," *IFAC Proc. Volumes*, vol. 41, no. 2, pp. 1697 – 1702, 2008.

[2] L. Bascetta and P. Rocco, "End-point vibration sensing of planar flexible manipulators through visual servoing," *Mechatronics*, vol. 16, no. 3-4, pp. 221 – 232, 2006.

[3] F. Chaumette and S. Hutchinson, "Visual servo control part ii: advanced approaches," *IEEE Robot. Autom. Mag.*, vol. 14, no. 1, pp. 109 – 118, Mar. 2007.

[4] J. Henikl, W. Kemmetmüller, and A. Kugi, "Modeling and control of a mobile concrete pump," *IFAC Proc. Volumes*, vol. 46, no. 5, pp. 91 – 98, 2013.

[5] P. Cheng and B. Oelmann, "Joint-angle measurement using accelerometers and gyroscopes - a survey," *IEEE Trans. Instrum. Meas.*, vol. 59, no. 2, pp. 404 – 414, Feb. 2010.

[6] J. Vihonen, J. Honkakorpi, J. Tuominen, J. Mattila, and A. Visa, "Linear accelerometers and rate gyros for rotary joint angle estimation of heavy-duty mobile manipulators using forward kinematic modeling," *IEEE/ASME Trans. Mechatron.*, vol. 21, no. 3, pp. 1765 – 1774, June 2016.

[7] H. A. Cronje and J. Gouws, "Inertial measurement system for the position control of a flexible robot arm," in *Proc. of 8th Mediterranean Electrotechnical Conf.*, vol. 2, May 1996, pp. 1141 – 1144.

[8] A. D. Luca, D. F. Schröder, and M. Thümmel, "An acceleration-based state observer for robot manipulators with elastic joints," in *IEEE Int. Conf. on Robot. Autom.*, Apr. 2007, pp. 3817 – 3823.

[9] W. Chen and M. Tomizuka, "Direct joint space state estimation in robots with multiple elastic joints," *IEEE/ASME Trans. Mechatron.*, vol. 19, no. 2, pp. 697 – 706, Apr. 2014.

[10] B. Siciliano and O. Khatib, *Springer Handbook of Robotics*. Springer-Verlag, 2007.

[11] G. Zhu, T. Lee, and S. Ge, "Tip tracking control of a single-link flexible robot: A backstepping approach," *Dynamics and Control*, vol. 7, no. 4, pp. 341 – 360, October 1997.

[12] L. Bascetta, G. Ferretti, and B. Scaglioni, "Closed-form Newton-Euler dynamic model of flexible manipulators," *Robotica*, vol. 35, no. 5, 2017.

[13] W.-H. Zhu, *Virtual Decomposition Control - Toward Hyper Degrees of Freedom Robots*. Springer-Verlag, 2010.